THE JOURNAL OF PHYSICAL CHEMISTRY C
A JOURNAL OF THE AMERICAN CHEMICAL SOCIETY

pubs.acs.org/JPCC

Article

Explanation of the Opposing Shifts in the Absorption Edge and the Optical Resonance in $CuFeS_2$ Nanoparticles

Yuan Yao, Santu Biswas, Minsoo Kang, Maytal Caspary Toroker,* and Richard D. Robinson*

Cite This: *J. Phys. Chem. C* 2022, 126, 5592−5597

Read Online

ACCESS | Metrics & More | Article Recommendations | Supporting Information

ABSTRACT: Size-dependent change of the electronic band structure is one of the key features of nanoparticles in the quantum confinement region. $CuFeS_2$ nanoparticles have a strong absorption feature in the visible region that has, controversially, been described as neither an excitonic transition nor a free carrier plasmon oscillation. Instead, the absorption feature in $CuFeS_2$ nanoparticles has been attributed to quasi-static optical resonances from inter-band transitions between the valence band (VB), intermediate band (IB), and conduction band (CB). As such, we hypothesized that the feature should be subject to quantum confinement effects through modification of the electronic bands. In this paper, we show experimentally that the optical resonance absorption peak red-shifts and the optical band gap blue-shifts as the particle size decreases. Through density functional theory (DFT) and the tight binding (TB) modeling, we elucidate the size dependence of the band structure, especially focusing on the change in the IB. Using a Lorentzian oscillator optical model to simulate the absorption spectrum with inputs from the DFT-calculated band structure and band shifts from the TB model, we find that the size-dependent shifts of the optical resonance peak position in $CuFeS_2$ are due to a tri-band quantum confinement effect that results in both the VB to IB and IB to CB gap expansion that accompanies a decrease in particle size. We also find that the transitions between the IB and CB play only a minor role in the optical spectrum. Moreover, the linear optical Lorentzian model predicts that the optical resonance peak is tunable across the visible range by partially filling the IB, lowering the CB, or expanding the IB.

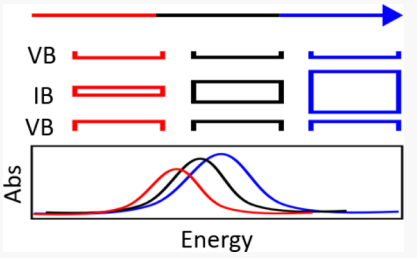

INTRODUCTION

$CuFeS_2$ nanoparticles are novel dielectric materials that possess a prominent plasmon-like absorption feature in the visible region (~2.5 eV), giant optical nonlinearity, and have the potential for post-synthetic wavelength tuning. Despite having optical properties similar to those of other semiconductor plasmonic materials, the quasi-static optical resonance in $CuFeS_2$ is contributed by collective electronic transitions between filled and unfilled states rather than by a free carrier oscillation.[1−4] This $CuFeS_2$ optical resonance feature shows a small red shift as the particle size decreases. For example, the optical resonance peak shifts from 2.53 to 2.34 eV as the particle size decreases from 12 to 7.5 nm.[1] Conversely, studies report blue shifts in the band gap with a decrease in size: the band gap in $CuFeS_2$ has been reported to increase from 0.52 to 0.81 eV as the particle size decreases from 15 to 3 nm.[3] This contrasting trend between the shifts in the optical band gap and the optical resonance feature is particularly interesting since the optical resonance feature is mainly contributed by the collective electronic transitions between the valence and intermediate bands (IBs),[4,5] and an increased band gap typically implies blue shifts in optical features. For the $CuFeS_2$ absorption feature, however, the opposite trend is observed. The abnormal dependence of the optical resonance position on the particle size for $CuFeS_2$ could be due to its special tri-band structure, but this premise has never been proven.

To investigate the size dependence of $CuFeS_2$ optical resonance, we combined experimental data from our colloidal nanoparticle synthesis with density functional theory (DFT) and optical spectra calculations. Different sizes of $CuFeS_2$ nanoparticles ranging from 14.6 to 4.9 nm are synthesized and characterized using transmission electron microscopy (TEM), electron diffraction (ED), and UV−Vis absorption spectroscopy. As the particle size decreases, a small red shift in the absorption is observed, while the optical band gap energy extracted from the absorption spectrum gradually increases by 0.34 eV. To explore the quantum confinement effect in this tri-band semiconductor system, DFT calculations are conducted for three different sizes of $CuFeS_2$ clusters as well as bulk $CuFeS_2$, and the band-edge shift is analyzed. A simple tight binding (TB) model is introduced to qualitatively explain the electronic structure change with size. Finally, a Lorentzian linear optical model is used to simulate the absorption spectrum for different sizes of $CuFeS_2$ nanoparticles. The optical simulations find a red shift in the optical resonance

Received: September 8, 2021
Revised: March 4, 2022
Published: March 21, 2022

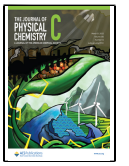

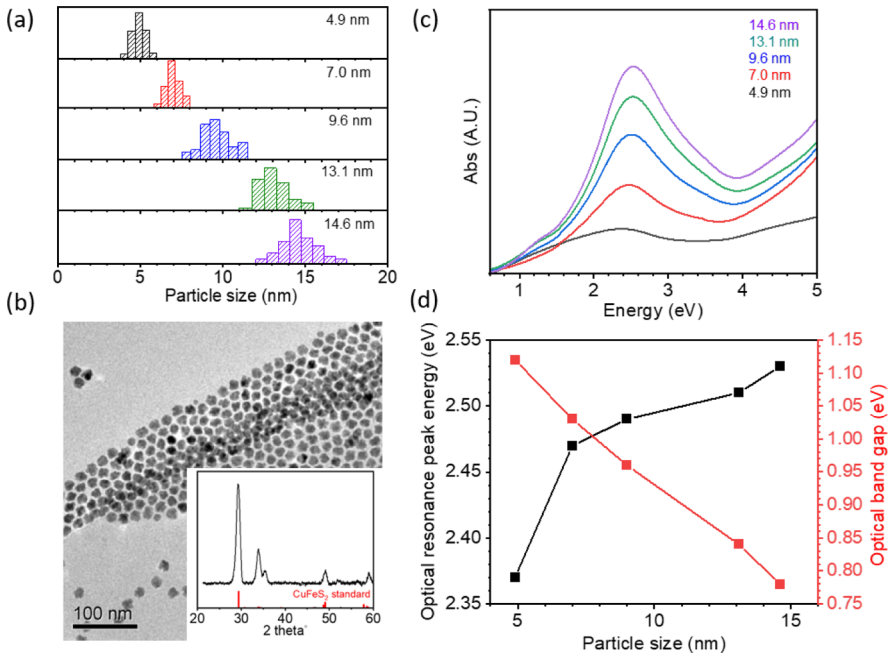

Figure 1. Experimental characterization of the size series of $CuFeS_2$ nanoparticles. (a) Size distribution histograms for the five particle sets: 4.9 nm ± 8.2%, 7.0 nm ± 6.6%, 9.0 nm ± 9.3%, 13.1 nm ± 7.1%, and 14.1 nm ± 7.6%. (b) TEM image of the 14.6 nm $CuFeS_2$ nanoparticles with the corresponding electron diffraction pattern as the inset. [Red bars in the inset correspond to chalcopyrite standard PDF#01-070-8495 (RDB).] (c) UV−Vis absorption spectra for the five different sizes of $CuFeS_2$ nanoparticles. As the particle size decreases, the absorption peak shifts from 2.53 eV (14.6 nm diameter) to 2.37 eV (4.9 nm). (d) Optical resonance peak energy (left *y*-axis) and optical band gap energy (right *y*-axis) extracted by linear extrapolation of the absorption edge, for the five nanoparticle samples.

feature as the particle size decreases, consistent with the experiment result. The results indicate that the size-dependent optical resonance behavior in $CuFeS_2$ is due to a tri-band quantum confinement effect. Moreover, using our linear optical model to extend the predictions for these systems, we find large peak shifts and the emergence of new peaks in cases where the IB upper edge shifts, the conduction band (CB) lower edge shifts, or there is a partial filling of the IB.

RESULTS AND DISCUSSION

A size range of $CuFeS_2$ pure-phase nanoparticles (4.9 nm ± 8.2%, 7.0 nm ± 6.6%, 9.0 nm ± 9.3%, 13.1 nm ± 7.1%, and 14.1 nm ± 7.6%) are synthesized through the hot injection of a sulfur precursor (penicillamine dissolved in oleylamine and octadecene) into a metal precursor ($FeCl_3$ and CuI dissolved in oleylamine and octadecene) at 180 °C. The particle size is controlled by varying the reaction time (experimental details in the Supporting Information). The particle size distribution for the five sets of particles indicates that all particles are monodisperse (less than 10% relative standard deviation) (Figure 1a). TEM images and ED patterns show that the particles are a pure chalcopyrite phase ($CuFeS_2$, PDF #01-070-8495) with good monodispersity (in Figure 1b, the data are shown for the largest $CuFeS_2$ nanoparticles of 14.6 nm ± 8.3%, also see Figures S1 and S2). A broad optical resonance peak is present in the UV−Vis spectrum around 2.5 eV that gradually increases in intensity as the particle size increases (Figure 1c). A relatively small energy decrease in the optical absorption resonance peak (from 2.53 to 2.37 eV) is observed despite the large particle size decrease from 14.6 to 4.9 nm. The optical band gaps for the five samples are extracted from the absorption spectrum (Figure S3a) and plotted against the optical resonance peak energy for the size range of nanoparticles (Figure 1d). As the particle size decreases, the optical band gap energy gradually increases from 0.78 eV (for the nanoparticle with a 14.6 nm diameter) to 1.12 eV (4.9 nm), while the optical resonance peak energy decreases from 2.53 eV (14.6 nm) to 2.37 eV (4.9 nm); an absorption peak red shift of 0.16 eV for an optical band gap energy blue shift of 0.34 eV. Our size-dependent resonance data align well with other $CuFeS_2$ size studies. For example, Ghosh et al.[1] found that as the particle size decreased from 12 to 7.5 nm, the $CuFeS_2$ optical resonance peak red-shifts from 2.53 to 2.34 eV, and Tauc analysis shows that the optical bandgap expands from 0.64 to 1.18 eV. To be noted, in the case of $CuFeS_2$, both the IB and CB are available to transition from the valence band (VB) within the visible energy range. Thus, although we are fitting a band-edge rise below 2.0 eV, the absorption tail from VB−CB transitions makes a small contribution to the absorption edge, which blue-shifts the extracted optical band gap. To illustrate this point, we set up a simple two-band system for two different band configurations. Both cases had a 1 eV band gap between the VB and CB, but the conduction bandwidth was varied from narrow to wide (0.5 eV vs 2.0 eV) (Figure S4 and Table S2). The absorption spectrum is simulated using the linear optical Lorentzian model, and the corresponding optical band gap energies are extracted by the Tauc plot method. The extracted optical band gap energy is 1.50 eV in the narrow CB case and 2.87 eV in the wide CB case. The larger optical band gap energy extrapolated in the wide CB case is due to the additional electronic transitions to higher unfilled states.

The ~2.5 eV absorption feature for $CuFeS_2$ has previously been interpreted as either a plasmon or an optical resonance (collective electronic transitions from the VB to higher bands).[2,4] Thin-film sample (see Hall measurement details in

https://doi.org/10.1021/acs.jpcc.1c07956
J. Phys. Chem. C 2022, 126, 5592−5597

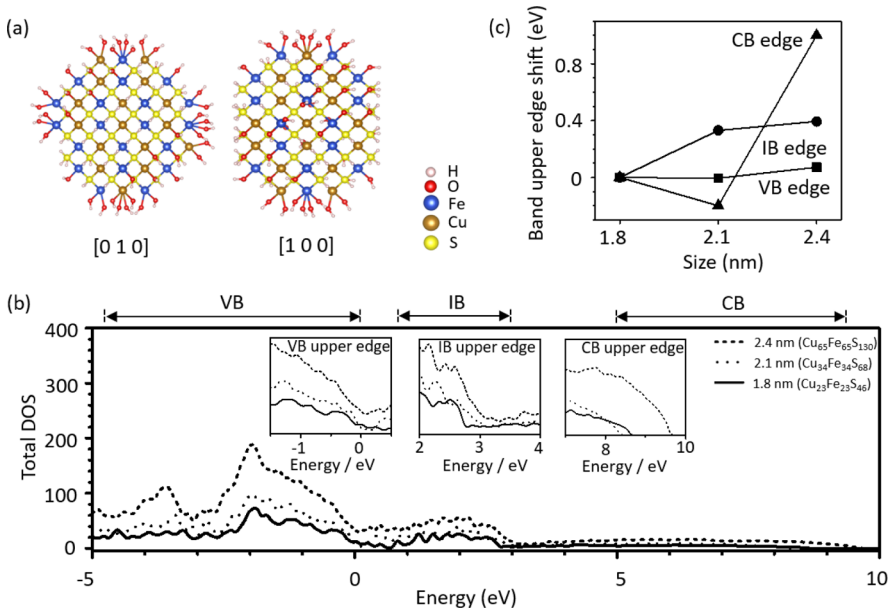

Figure 2. DFT calculations to estimate shifts in electronic band edges. (a) Atomic structure for H- and OH-capped $Cu_{34}Fe_{34}S_{68}$ clusters used in the DFT calculations. (b) Total density of states for three different sizes of $CuFeS_2$ clusters—1.8 nm ($Cu_{23}Fe_{23}S_{46}$), 2.1 nm ($Cu_{34}Fe_{34}S_{68}$), and 2.4 nm ($Cu_{65}Fe_{65}S_{130}$)—with insets showing higher magnification details of the VB, IB, and CB upper edge. (Note: IB and CB lower edges are determined from the bulk $CuFeS_2$ result in Figure S5.) (c) Band upper edge shift for VB, IB, and CB with respect to cluster size. The IB and CB upper edge decreases 0.4 and 1.0 eV, respectively, with the cluster size decrease, but the VB upper edge remains constant.

the Supporting Information) shows a hole concentration of 1.2 × 10^{16} cm^{-3}, which is much smaller than the free carrier density (10^{22} to 10^{23} cm^{-3}) necessary to produce plasmonic absorption in the visible range, as found in metal plasmonic nanoparticles such as gold.[6,7] Previous studies of $CuFeS_2$ have reported an higher carrier concentration of up to 10^{18} cm^{-3},[8,9] but even these values are orders of magnitude lower than what would be required to produce the ∼2.5 eV absorption band, implying that this absorption feature for $CuFeS_2$ is a result of collective inter-band transitions and not free carriers (see free carrier calculation in the Supporting Information). Since our nanoparticles are close to the de Broglie wavelength of $CuFeS_2$ (∼2.2 nm), the change in band structure due to size-dependent shifts could be the cause for the optical resonance shifts. To clarify the relationship between the optical resonance size dependence with band structure quantum confinement, we employed DFT calculations and a TB model. From the results of the size-dependent band structure from the DFT and TB calculations, we simulate the optical spectrum for different size $CuFeS_2$ nanoparticles and predict the optical resonance shift with respect to the particle size change using a Lorentzian oscillator model for the optical transitions.

To evaluate the dependence of band structure on particle size, we perform DFT calculations for bulk $CuFeS_2$ and three different sizes of $CuFeS_2$ nanoparticles: 1.8 nm ($Cu_{23}Fe_{23}S_{46}$), 2.1 nm ($Cu_{34}Fe_{34}S_{68}$), and 2.4 nm ($Cu_{65}Fe_{65}S_{130}$). Hydrogen and hydroxyl groups are bonded to the sulfur and metal surface atoms to remove the dangling bonds and damp the surface states (2.1 nm $Cu_{34}Fe_{34}S_{68}$ shown in Figure 2a).[10] (More computational details about the DFT calculation can be found in the Supporting Information.) The total density of states (DOSs) for three sizes of clusters ($Cu_{23}Fe_{23}S_{46}$, $Cu_{34}Fe_{34}S_{68}$, and $Cu_{65}Fe_{65}S_{130}$) are shown in Figure 2b, with inset plots highlighting the upper edge of the VB, IB, and CB. From the DOS plots, it is clear that the upper edges of the IB and CB shrink to lower energy as the size of the cluster decreases. We extract the upper edges of the VB and IB by linear fitting (Figures S8 and 2c) and directly read the upper edge of the CB (as it is free of noise from surface states). The upper edge of the VB remains nearly constant as the cluster size changes. Conversely, the IB upper edge decreases by 0.4 eV (3.22 to 2.82 eV), and the CB upper edge decreases by 1.0 eV (9.6 to 8.6 eV) as the cluster size decreases from 2.4 to 1.8 nm. Concerning the lower edges of the IB and CB: significant noise hampers the ability to track their position (Figure S6). Based on previous DFT reports on similar-sized $CuFeS_2$ clusters, the DOS noise in between bands is mainly due to surface states.[10] To confirm that the extra DOS comes from the surface states, we compared the inner cluster versus the full cluster partial DOS for the three elements (Figure S7), and the inner cluster partial DOS shows a significantly decreased noise in between bands. It will be shown later that information about the lower band edges can be extracted from combining information from the TB model, the Lorentzian oscillator model, and experimental data. In summary, the cluster DFT results indicate that the VB upper edge position is independent of the cluster size, but the upper edge of the IB and CB bands shifts to a lower energy as the cluster size decreases.

To study the position of the IB and CB lower edges with respect to the cluster size and to examine the band expansion in the IB upper edge, we employ a TB model. Moreover, the TB model enables flexibility in changing the electronic structure of the tri-band material by tuning the TB parameters and thereby allows correlation between the tri-band electronic structure and the resonance peak position. The TB model assumes that only nearby orbitals interact and the TB model uses multiple simplified sets of wavefunctions to calculate the electronic band structure for solids. The TB model allows semi-quantitative calculations of the band structure for a large number of atoms (e.g., TB can incorporate more than 100,000 atoms compared to less than 1000 for DFT). Considering that our smallest nanoparticle sample has ∼10,000 atoms (3.3 nm),

https://doi.org/10.1021/acs.jpcc.1c07956
J. Phys. Chem. C 2022, 126, 5592−5597

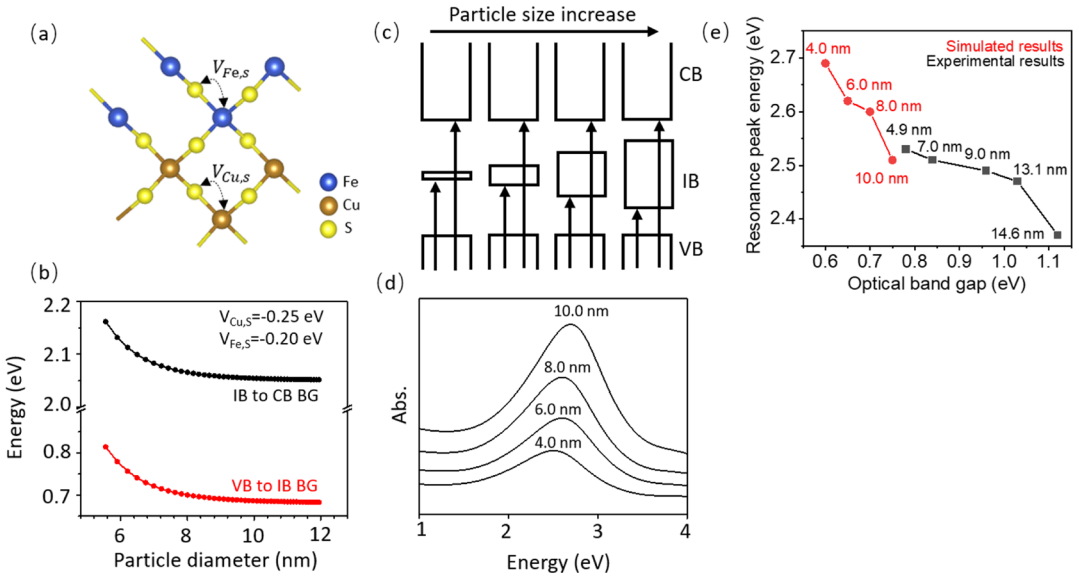

Figure 3. TB and the linear optical models to simulate electronic bands and optical properties. (a) Schematic of the $CuFeS_2$ crystal structure to illustrate the location of the hopping integrals $V_{Cu,S,}$ and $V_{Fe,S}$ used in the TB calculations. (b) Calculated band gap (BG) size change with decreased particle diameter (assuming a spherical particle model) from the TB model. Values used for inter-band hopping energies: $V_{Fe,S}$ = −0.25 eV and $V_{Cu,S}$ = −0.20 eV (corresponding to the best fit to the bulk DFT result when particle size = 10 nm). (c) Schematic for the four band structures used for the linear Lorentzian oscillator model. The four configurations represent band structures for four different-sized particles (left to right: 4, 6, 8, and 10 nm). (d) Simulated absorption spectra from the Lorentzian oscillator model using the four configurations of band structures for the four different particle sizes. The spectra show that the peak of the optical resonance red-shifts as the particle size decreases. (e) Plot of experimentally determined optical resonance peak energy vs optical band gap energy (black) and simulated absorption peak energy vs optical band gap energy (red). The optical resonance peak energy decreases from 2.53 to 2.37 eV as the optical band gap energy increases from 0.78 to 1.12 eV. For the simulation, the absorption peak energy decreases from 2.69 to 2.51 eV as the VB to IB band gap increases from 0.6 to 0.75 eV, showing a similar trend as the experimental data.

the TB method is suitable for modeling the size-dependent effects. Solutions for the wavefunctions are extracted by solving the TB Hamiltonian matrix, which consists of diagonal terms [unhybridized orbital energy (E)] and off-diagonal terms [nearest orbital hopping energy (V)]. The inter-band hopping integrals $V_{Cu,S,}$ and $V_{Fe,S}$ account for the electron hopping between the nearest-neighbor copper to sulfur and iron to sulfur orbital, respectively. The intra-band hopping integrals $V_{Cu,Cu}$, $V_{Fe,Fe}$, and $V_{S,S}$ are used to account for the copper to copper, iron to iron, and sulfur to sulfur orbital interactions, respectively. The band-center energy of the VB, IB, and CB is taken from our bulk DFT calculation (Figure S5) and used as E_{Cu}, E_{Fe}, and E_S since the main contributors for the VB, IB, and CB are copper 3d, iron 3d, and sulfur 2p orbitals, respectively (Table S3). The interband hopping terms (0.2 eV) are extracted as 1/4 of the IB bandwidth from the bulk DFT calculation.[11]

For the inter-band hopping energy ($V_{Cu,S}$ and $V_{Fe,S}$), literature reports values ranging from −0.01 to −0.65 eV.[12,13] We used a range of values (from −0.10, −0.05 eV to −0.65, −0.60) for the $V_{Fe,S}$ and $V_{Cu,S}$, respectively. The lower energy for $V_{Fe,S}$ (e.g., −0.25 vs −0.20 eV with respect to zero energy) is due to the higher Fe−S binding energy compared to Cu−S. A schematic for the full TB matrix is shown in Figure S9, and a listing of all the parameters used is tabulated in Table S3.

Based on the fact that the VB, IB, and CB are dominated by Cu, Fe, and S DOS, respectively, the IB−CB and VB−CB interactions are determined by the hopping integral $V_{Fe,S,}$ and $V_{Cu,S}$, which are the focus of our TB model (Figure 3a). For inter-band hopping energy of $V_{Fe,S}$ = −0.25 eV and $V_{Cu,S}$ = −0.20 eV, we find that as the number of atoms decreases, both the VB−IB band gap and the IB−CB band gap expand by ∼0.15 eV (0.70 to 0.82 eV and 2.07 to 2.16 eV for the VB−IB and IB−CB band gap, respectively, as the particle size decreases from 10 to 4 nm) (Figure 3b). This trend (increasing band gap as the particle size decreases) is consistently observed through the range of $V_{Fe,S}$ and $V_{Cu,S}$ values used (−0.10, −0.05; −0.25, −0.20; −0.35, −0.30; −0.45, −0.40; −0.55, −0.50; and −0.65, −0.60 eV) (Figure S10). The band gap expansion as the particle size decreases is a result of bandwidth shrinkage as the number of states decreases; this result is consistent with the classical quantum confinement calculations for two-band systems. Based on our DFT results, the VB upper edge is independent of size. Thus, the increase of the VB−IB band gap as the particle size decreases has to be the result of the increasing edge position of the IB lower edge. Concerning the IB−CB band gap, we know that the IB upper edge decreases as the particle size decreases, but the lower edge of the CB can increase, decrease, or stay constant with respect to the particle size. To investigate the IB−CB band gap contribution to the formation of the optical resonances, we created models with three different band structures—the lower edge of the CB increases, decreases, or stays constant with respect to the particle size—and modeled their corresponding size dependence of the absorption peak position using the linear optical Lorentzian model.

Optical resonance occurs when the excitation light is at the energy defined by the gap between filled and unfilled states. In the case of the quasi-static resonance in $CuFeS_2$, the sum of all the individual photon-excited electronic transitions from the VB to the IB and CB contributes to the overall absorption spectrum. Our DFT calculations (see the Supporting Information) show that the Fe 3d, Cu 3d, and S 2p orbitals

https://doi.org/10.1021/acs.jpcc.1c07956
J. Phys. Chem. C 2022, 126, 5592−5597

have overlaps in all three bands, which permit the inter-band transition between the valence to the IB and CB.[4,5] The electronic transitions can be modeled using a linear optical Lorentzian oscillator model, which assumes that the binding force between the electron and core can be described by a spring constant. To obtain the dielectric function, all electronic transitions from the VB to the unfilled states in the IB and CB are considered. The Mie theoretic equation (generally applicable to all types of materials) is used for the calculation of the optical spectrum, specifically for the absorption cross-sectional σ.[14]

$$\sigma = \zeta \frac{\varepsilon_m \varepsilon_i}{(\varepsilon_r + 2\varepsilon_m)^2 + \varepsilon_i^2}$$

$$\zeta = 24\pi^2 R^3 \sqrt{\varepsilon_m}/\lambda$$

R: particle radius; λ: excitation wavelength; ε_m: permittivity of the medium; ε_r: real permittivity; and ε_i: imaginary permittivity.

As input parameters to refine the model, we can use the band structure size dependence predicted by DFT and the TB model. The band position for the 10 nm nanoparticle is taken from the bulk DFT calculation (Figure S5), and the amount of band shrinkage is estimated from the TB model (~0.15 eV change of the band gap between the largest and the smallest particle) (all details for the linear optical model can be found in the Supporting Information.). As mentioned previously, we examined three different band structure configurations for the CB lower edge: increasing, decreasing, or remaining constant with respect to the particle size change (Figure S11 and Table S4). Figure 3c shows the schematic of the band structures for four different sizes of particles for the case of keeping the CB lower edge constant. As the particle size decreases from 10 to 4 nm, the IB width shrinks from 1.2 to 0.9 eV, increasing the VB−IB band gap from 0.60 to 0.75 eV and the IB−CB band gap from 2.00 to 2.15 eV (as shown in the TB model). The resulting spectrum for our linear optical Lorentzian model (Figure 3d) finds that the optical resonance peak energy decreases (from 2.69 to 2.51 eV) as the particle size decreases (by shrinking the IB), which is consistent with the experimental results. Interestingly, in the other two cases (IB−CB band gap increase, decrease), we also found that the optical resonances shift to lower energy as the particle size decreases (Figure S11b,c), which indicates that the IB−CB transition makes little contribution to the optical resonances in $CuFeS_2$.

The absorption peak energies are plotted as a function of the optical band gap energies for both experimental and simulated data, shown in Figure 3e. For the simulated data, the VB−IB gap values are used as the optical band gap. The trends in both plots are similar: a concomitant expansion of the optical band gap energy with a decrease in the optical resonance peak energy. Comparison between the trends in experimental and simulated optical resonance peak energy and optical band gap energy finds a strong correlation, which indicates that the quasi-static resonance size dependence in $CuFeS_2$ nanoparticles is caused by the band structure change through a quantum confinement effect.

Apart from varying the size of the nanoparticle, the $CuFeS_2$ optical resonance peak can be tuned by other means including charging the materials (filling the IB), anionic doping (generating donor states, thereby expanding or shrinking the CB), and cationic doping (change in the upper edge of the IB). Using the linear optical Lorentzian model, we investigate the optical resonance change under three conditions: (1) partial filling of the IB, (2) lowering of the CB lower edge with increased DOSs, and (3) increase of the IB upper edge (see Figure S12 and all input parameters in Table S6). Partial filling of the IB causes the original 2.7 eV resonance peak to decrease in intensity and a 1.6 eV resonance peak to appear and increase in intensity as the electrons fill the IB (Figure S12a). The new, lower energy resonance peak is caused by the electronic transition between the filled IB state and the unfilled IB state. The new absorption band is broader than the pure $CuFeS_2$ case, which could augment the functionality of this material to block a greater range of the visible light spectrum. Lowering of the CB lower edge with increased DOSs also reduces the original 2.7 eV resonance peak intensity and introduces a new peak at 4.4 eV, which is caused by electronic transitions from the VB to the higher energy CB states (Figure S12b). This case would increase the functionality of the material by blocking more UV light. In both cases, the decreased intensity in the 2.7 eV resonance peak is due to the reduced inter-band transition contribution. Expansion of the IB higher edge leads to the shift of the resonance peak to a higher energy (2.7 to 4.1 eV) (Figure S12c). The resonance peak energy shift is caused by the electronic transition to the IB high-energy states. These simulation results show that $CuFeS_2$ is a potentially useful optical material with tunable absorption across the whole visible and UV range.

CONCLUSIONS

In this paper, we synthesize a size series of $CuFeS_2$ and find that as the particle size decreases (14.6 to 4.9 nm), the optical resonance peak red-shifts (2.53 to 2.37 eV) accompanied by an optical band gap energy increase (0.78 to 1.12 eV). The carrier density analysis along with the linear optical Lorentzian model proves that the optical resonance in $CuFeS_2$ is mainly contributed by the inter-band transitions. We employ DFT and the TB model to simulate the $CuFeS_2$ nanoparticle band structure size dependence and find that both the VB−IB and IB−CB band gaps expand as the particle size decreases. Using the simulated band structure as inputs, we used the linear optical Lorentzian model to study the resonance size dependence. The simulated optical spectrum shows that the resonance peak energy decreases and the optical band gap increases as the particle size decreases. The simulated results align well with our experimental results and prove that the abnormal dependence of the optical resonance position on the particle size for $CuFeS_2$ is due to the existence of the tri-band structure. Moreover, we extend our linear optical Lorentzian model to the case of IB upper edge shifts, CB lower edge shifts, and partial filling of the IB. Partial filling of the IB and lowering of the conduction lead to damping of the original 2.7 resonance peak and formation of new resonance peaks at 1.6 and 4.4 eV, respectively. Expansion of the IB higher edge leads to the shift of the resonance peak to a higher energy (2.7 to 4.1 eV). These results show that the resonance absorption band in $CuFeS_2$ is tunable across the visible range and into the UV.

ASSOCIATED CONTENT

Supporting Information

The Supporting Information is available free of charge at https://pubs.acs.org/doi/10.1021/acs.jpcc.1c07956.

https://doi.org/10.1021/acs.jpcc.1c07956
J. Phys. Chem. C 2022, 126, 5592−5597

Additional experimental details and details and methods for the DFT, TB, and optical simulation (PDF)

AUTHOR INFORMATION

Corresponding Authors

Maytal Caspary Toroker − *Department of Materials Science and Engineering, Israel Institute of Technology, Haifa 3200003, Israel; The Nancy and Stephen Grand Technion Energy Program Technion—Israel Institute of Technology, Haifa 3200003, Israel;* orcid.org/0000-0003-1449-2977; Email: maytalc@technion.ac.il

Richard D. Robinson − *Department of Materials Science and Engineering, Cornell University, Ithaca, New York 14853, United States;* orcid.org/0000-0002-0385-2925; Email: rdr82@cornell.edu

Authors

Yuan Yao − *Department of Materials Science and Engineering, Cornell University, Ithaca, New York 14853, United States;* orcid.org/0000-0002-4784-2753

Santu Biswas − *Department of Materials Science and Engineering, Israel Institute of Technology, Haifa 3200003, Israel*

Minsoo Kang − *Department of Materials Science and Engineering, Cornell University, Ithaca, New York 14853, United States*

Complete contact information is available at: https://pubs.acs.org/10.1021/acs.jpcc.1c07956

Notes

The authors declare no competing financial interest.

ACKNOWLEDGMENTS

This work was supported in part by the National Science Foundation (NSF) under award numbers CMMI-1941135 and DMR-2003431. This work made use of the Cornell Center for Materials Research Shared Facilities, which are supported through the NSF MRSEC program (DMR-1719875). This research was also supported by a grant from the United States-Israel Binational Science Foundation (BSF), Jerusalem, Israel, and the Nancy and Stephen Grand Technion Energy Program (GTEP).

REFERENCES

(1) Ghosh, S.; et al. Colloidal $CuFeS_2$ Nanocrystals: Intermediate Fe d-Band Leads to High Photothermal Conversion Efficiency. *Chem. Mater.* **2016**, *28*, 4848−4858.

(2) Sugathan, A.; Bhattacharyya, B.; Kishore, V. V. R.; Kumar, A.; Rajasekar, G. P.; Sarma, D. D.; Pandey, A. Why Does $CuFeS_2$ Resemble Gold? *J. Phys. Chem. Lett.* **2018**, *9*, 696−701.

(3) Bhattacharyya, B.; Pandey, A. $CuFeS_2$ Quantum Dots and Highly Luminescent $CuFeS_2$ Based Core/Shell Structures: Synthesis, Tunability, and Photophysics. *J. Am. Chem. Soc.* **2016**, *138*, 10207−10213.

(4) Gaspari, R.; Della Valle, G.; Ghosh, S.; Kriegel, I.; Scotognella, F.; Cavalli, A.; Manna, L. Quasi-Static Resonances in the Visible Spectrum from All-Dielectric Intermediate Band Semiconductor Nanocrystals. *Nano Lett.* **2017**, *17*, 7691−7695.

(5) Yao, Y.; Bhargava, A.; Robinson, R. D. Fe Cations Control the Plasmon Evolution in $CuFeS_2$ Nanocrystals. *Chem. Mater.* **2021**, *33*, 608−615.

(6) Alvarez, M. M.; Khoury, J. T.; Schaaff, T. G.; Shafigullin, M. N.; Vezmar, I.; Whetten, R. L. Optical Absorption Spectra of Nanocrystal Gold Molecules. *J. Phys. Chem. B* **1997**, *101*, 3706−3712.

(7) Luther, J. M.; Jain, P. K.; Ewers, T.; Alivisatos, A. P. Localized surface plasmon resonances arising from free carriers in doped quantum dots. *Nat. Mater.* **2011**, *10*, 361−366.

(8) Liang, D.; Ma, R.; Jiao, S.; Pang, G.; Feng, S. A facile synthetic approach for copper iron sulfide nanocrystals with enhanced thermoelectric performance. *Nanoscale* **2012**, *4*, 6265.

(9) Bastola, E.; Bhandari, K. P.; Subedi, I.; Podraza, N. J.; Ellingson, R. J. Structural, optical, and hole transport properties of earth-abundant chalcopyrite (CuFeS2) nanocrystals. *MRS Commun.* **2018**, *8*, 970−978.

(10) Thinius, S.; Bredow, T. Spectroscopic Properties of Chalcopyrite Nanoparticles. *J. Phys. Chem. C* **2019**, *123*, 3216−3225.

(11) Caspary, M.; Peskin, U. Site-directed deep electronic tunneling through a molecular network. *J. Chem. Phys.* **2005**, *123*, 151101.

(12) Andersen, O. K.; Jepsen, O. Explicit, First-Principles Tight-Binding Theory. *Phys. Rev. Lett.* **1984**, *53*, 2571−2574.

(13) Xie, Y.; Blackman, J. A. Tight-binding model for transition metals: From cluster to solid. *Phys. Rev. B: Condens. Matter Mater. Phys.* **2001**, *63*, 125105.

(14) Olson, J.; Dominguez-Medina, S.; Hoggard, A.; Wang, L.-Y.; Chang, W.-S.; Link, S. Optical Characterization of Single Plasmonic Nanoparticles. *Chem. Soc. Rev.* **2015**, *44*, 40−57.